

# Modeling hairy root tissue growth in in vitro environments using an agent-based, structured growth model

Felix Lenk · Almuth Sürmann · Patrick Oberthür ·  
Mandy Schneider · Juliane Steingroewer ·  
Thomas Bley

Received: 16 July 2013 / Accepted: 31 October 2013 / Published online: 12 November 2013  
© Springer-Verlag Berlin Heidelberg 2013

**Abstract** An agent-based model for simulating the in vitro growth of *Beta vulgaris* hairy root cultures is described. The model fitting is based on experimental results and can be used as a virtual experimentator for root networks. It is implemented in the JAVA language and is designed to be easily modified to describe the growth of diverse biological root networks. The basic principles of the model are outlined, with descriptions of all of the relevant algorithms using the ODD protocol, and a case study is presented in which it is used to simulate the development of hairy root cultures of beetroot (*Beta vulgaris*) in a Petri dish. The model can predict various properties of the developing network, including the total root length, branching point distribution, segment distribution and secondary metabolite accumulation. It thus provides valuable information that can be used when optimizing cultivation parameters (e.g., medium composition) and the cultivation environment (e.g., the cultivation temperature) as well as how constructional parameters change the morphology of the root network. An image recognition solution was used to acquire experimental data that were used when fitting the model and to evaluate the agreement between the simulated results and practical experiments. Overall, the case study simulation closely reproduced experimental results for the cultures grown under equivalent conditions to those assumed in the simulation. A 3D-

visualization solution was created to display the simulated results relating to the state of the root network and its environment (e.g., oxygen and nutrient levels).

**Keywords** Hairy roots · *Beta vulgaris* · Growth modeling · Plant cell tissue · Agent-based model

## Abbreviations

AVL	Adelson-Velski and Landis (tree)
CSV	Comma separated values
MFA	Metabolic flux analysis
MS	Murashige & Skoog
MSL	Mean segment length
ODE	Ordinary differential equation
OOM	Object oriented model
SSL	Single segment length (mm)
SSM	Single-way state machine
TBP	total number of branching points
TNS	Total number of segments
TRL	Total root length (mm)
TRV	Total root volume (mm <sup>3</sup> )
UML	Unified modeling language
VERN	Virtual experimentator for root networks
X	Biomass (g/L)

## Introduction

Plants produce a wide range of nutritionally, physiologically, and pharmaceutically important secondary metabolites. However, the scope for conventional industrial exploitation of these substances has historically been limited by environmental and geographical factors. The production of secondary metabolites in plant cell and tissue

F. Lenk (✉) · M. Schneider · J. Steingroewer · T. Bley  
Faculty of Mechanical Science and Engineering,  
Institute of Food Technology and Bioprocess Engineering,  
Technische Universität Dresden, Dresden, Germany  
e-mail: felix.lenk@tu-dresden.de

A. Sürmann · P. Oberthür  
Institute of Scientific Computing, Technische Universität  
Dresden, Dresden, Germany

cultures represents an alternative to classical methods for obtaining such compounds. This method enables year-round cultivation in bioreactors under optimized conditions, does not require the use of harmful substances such as pesticides, and can facilitate the product's approval by agencies such as the FDA and ESFA because of the well-defined culture conditions that are used. Hairy root cultures are plant cell cultures that have been manipulated using *Agrobacterium rhizogenes* and are particularly useful in the production of valuable secondary metabolites such as the red pigments known as the Betalains that were first identified in beetroots (*Beta vulgaris*). However, there are several important challenges associated with bioreactor cultivation and the process of screening for promising culture lines in Petri dishes, and these will have to be overcome to expand the scope of the bioreactor approach [1, 2].

In the past, many researchers have conducted systematic experimental campaigns to identify optimal conditions for the production of secondary metabolites using hairy root cultures. For example, Georgiev et al. [3] and Mukundan et al. [4] reported detailed investigations into the production and release of Betalains, Nussbaumer et al. [5] studied the use of hairy root cultures derived from *Datura candida* and Boschke et al. [6] investigated on colony formation and dense-branching growth of several yeasts. However, there is growing interest in the use of in silico modeling of growth processes as a way to identify improved culture conditions and media compositions, and for the development of bioreactor environments that are suitable for differentiated plant cultures. Metabolic flux analysis (MFA) has proven to be a powerful computational tool for investigating growth processes at the single cell level, and has been used to predict growth rates [7] as well as to elucidate the pathways involved in the production of target metabolites [8]. In addition, various purely macroscopic methods have been used to describe growth processes in hairy root cultures. For example, Ptashnyk et al. [9] used a macroscopic kinetic model to describe the absorption of nutrient substances through the cell wall, and Cloutier et al. [10] developed a kinetic model that describes the metabolism of nutrients by *Catharanthus roseus* and *Daucus carota* hairy root cultures to predict their growth and nutritional behavior under various conditions. Data generated using the latter model were used to support the up-scaling of a technical process. A population balance model that produces macroscopic forecasts concerning the formation and elongation of new root branches in hairy root cultures has been developed by Han et al. [11], and a comprehensive overview of the various mechanistic models for root network formation has been compiled by Dupuy et al. [12]. Although numerous approaches have been introduced for the analysis of specific isolated problems, there is currently

no general structured growth model that can quantitatively predict the growth processes of hairy roots in different cultivation systems on the macroscopic scale and in phenomenological terms [1].

While there is a lack of general predictive models for hairy root cultures, Walther et al. [13, 14] have conducted important experimental and theoretical investigations into mycelial growth in yeasts, and other studies have produced a mathematical model describing the regulatory mechanisms that govern yeast colony development [15]. In addition, a conclusive, partially object-oriented and agent-based approach known as BacSim has been developed by Kreft et al. [16] for the modeling of biofilm growth. Further elaboration of this model resulted in the development of the iDynoMiCS-suite [17], which uses a series of relatively simple individual elements to describe a much more complex overall process (in this case, biofilm growth and behavior). The work presented herein was inspired by this approach. The principal elements of our model data structure for simulating the evolution of morphological structure in hairy root cultures are based on the findings of Lindenmayer [18, 19], who introduced the so-called L-systems to describe filamentous growth processes. Aristid Lindenmayer in the late 1960s developed a mathematical description for the pattern formation during filamentous growth processes where cells change their state during cell division to form apical or banding patterns. With the finding to mathematically arrange agents to form a specific geometry it was possible to recreate nature-like plant shapes.

The aim of the studies reported herein was this to construct and fit a structured growth model for hairy root cultures and to simulate the development of their morphology to generate data that could be used to facilitate media optimization and structure determination, and to predict the sensitivity of cultures to morphological changes. This in turn should enable the design of new and improved bioreactors. The introduction of reliable predictive in silico methodologies should reduce the amount of experimental effort and laboratory time required to identify practical in vitro culture conditions.

The modeling and simulation tool developed in this work has been named the “Virtual Experimentator for Root Networks” (VERN). It consists of four different modules and is based on a single-way state machine (SSM):

1. Root- and organism-specific input data,
2. Recursive description and simulation algorithms, which are implemented using a SSM,
3. A 3D-visualization solution, which is used to display the simulated results,
4. A data output solution that generates time-step specific output files and output files containing information on

the overall outcome of the simulation to facilitate further analysis

The following sections describe the development of this comprehensive system for modeling the growth of dense root networks, and a practical application in the modeling of a beetroot (*Beta vulgaris*) hairy root culture.

## Materials and methods

It was necessary to collect and analyze experimental data concerning the growth of *Beta vulgaris* hairy roots to properly fit the model.

### Cultivation conditions

The aim of the work was to model the growth processes of *Beta vulgaris* hairy root cultures in Petri dishes. To provide reference data, cultures were grown in Petri dishes (92 mm diameter, Sarstedt 821473001), filled with Murashige & Scoog solid medium (MS, Duchefa Biochemistry, [20]) to a depth of  $7 \pm 1$  mm. The medium was supplemented with 30 g/L sucrose (Duchefa Biochemistry, Haarlem, The Netherlands), 5.5 g/L plant agar (Duchefa Biochemistry) and cultivated at 26 °C, using sub-cultivation intervals of 14 days each. The experiments were initiated by placing one *Beta vulgaris* hairy root sample (ca. 10 mm in length) in the center of each Petri dish. Six replicate cultures were established.

### Experimental data collection

As previously reported by Lenk et al. [21], experimental data for the modeling of the root network evolution were collected using a special tripod for Petri dish imaging in conjunction with an innovative method of automatic image recognition. Images of the Petri dishes containing the samples were recorded at 12 or 24 h intervals and analyzed to determine the cultures' growth rates and biomass production, and to monitor the intracellular accumulation of the red pigment Betalains. Image recognition was achieved by extracting the following parameters directly from each image:

- The length of every single segment (SSL),
- The segment volume,
- The width of each segment at both ends and in the middle,
- Branching point metrics, and
- The red pigment concentration (as a percentage) for each single segment.

In addition, global parameters such as the total root length (TRL), the total volume of the root network (TRV)

and global mean values for all relevant single parameters such as the mean segment length (MSL) were calculated during the image recognition process. The resulting data were processed further to generate the data required for model fitting (see “[Hairy root model architecture](#)”).

### Root- and organism-specific input data and environmental parameters

The output files produced by the image recognition system are used to determine the specific input data for the modeling process [21]. Two specific data types are collected by the image recognition system at each time-step: data on global evolution and changes in growth behavior, and segment-specific data.

Global data such as the total number of segments (TNS), total root length (TRL), total number of branching points (TBP), mean distance between adjacent branching points, pigment concentration in each segment and the direction of growth characterize the root system as a whole. Conversely, segment-specific data describe the evolution of individual segments and can be used to identify differences in the behavior and properties of younger and older segments with respect to characteristics such as length, width, volume and pigment concentration.

To characterize the functional development of each variable of interest, it was necessary to conduct several experiments using hairy roots growing under identical conditions (in terms of temperature, medium, timeframe, etc.) to determine the mean value of each characteristic per time-step. By plotting and interpolating the development of individual characteristic over time, we were able to characterize the root's functional behavior during the process of growing (i.e., to determine whether each characteristic changed in an exponential or linear fashion or remained constant).

In the programmed library, all characteristics were implemented with functional dependencies based on the results obtained through the analysis of experimental data to ensure that the simulated results would correspond well with real-world outcomes. This made it possible to adapt the program to describe all possible types of root growth because the functional behavior of the characteristics should be independent of the circumstances at hand, although the precise values required for each parameter will depend on the root organism being studied.

In practice, no natural process is perfectly reproducible; there is invariably a relatively high degree of variation due to random or uncontrolled factors. To account for this, a degree of variation was incorporated into the parameters governing every developmental process that was implemented in the model. The specific distribution of the

parameter values will depend on the root organism being studied and can be adjusted on a case-by-case basis.

To enable the simulation of experiments using different environments, parameters were introduced to describe the geometric form of the vessel containing the medium and the root organism as well as the chemical and physical composition of the medium. This makes it possible to simulate and visualize cultures grown in Petri dishes.

### Hairy root model architecture

To structure the problems mentioned above the authors used the standard protocol, ODD, introduced by Grimm et al. [22] to describe this agent-based model. The ODD generally consists of three blocks: overview, design concepts, and details. Applications of these blocks to the hairy root model can be found in the following three sub-chapters.

#### Overview

To model the growth behavior of complex root networks and the associated changes in morphology, it is necessary to determine the model system (assuming at  $t_{\text{equi}}$  that it is capable of unlimited growth to begin with) and to collect the subject-related experimental data to describe the relevant growth processes. In general, the growth of the root network as a whole can be described in terms of three separate processes [22, 23]:

- The formation of new tips and branching points
- Tip elongation
- Secondary thickening.

The complete model presented in this article is based on these three processes. Its derivation is described in the methods section, starting with the structure of the root- and organism-specific input data. These data originate from experimental results, and must be acquired before simulations can be conducted. This is followed by an outline of the developed model using the ODD-Framework by Grimm et al. [22] together with a description of relevant algorithms. The results of the simulations are visualized using an OpenGL library implemented in JAVA to display the data in 3D. To make the results scientifically useful, an output structure has been developed to facilitate further computation and other uses of the simulated results (see “[Time-step specific and overall output of simulation results for further computation](#)”).

To model the growth of hairy root plant tissue cultures, the authors used a discretely timed recursive description system which is solely based on the previous time-step. Figure 1 illustrates this approach in terms of stepping from time-step ( $t$ ) to time-step ( $t + 1$ ) horizontally. Vertically it

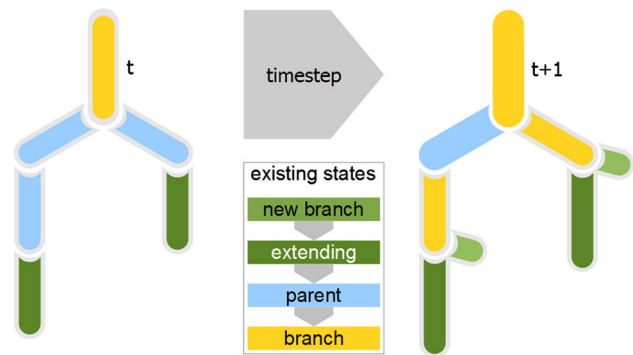


**Fig. 1** Principle overview of the simulation process, showing the recursive time-step controlled algorithm horizontally and the single-way state machine vertically

also explains the agent-based approach by incorporating the single-way state machine which describes the life stages of each agent. Single way state machines provide a solution to discretely connect a combination of input signals to the relevant set of output signals. The sets are grouped as stages that are being processed in a defined order with only one direction thus referring to the term single-way.

Every life stage is coded to a color: the formation of new branches on the tips of the root network is represented in bright green. Consequently, agents change to the next stage in dark green representing the growth on the tip of the root network. In order to make it possible for agents to form branches not only on the tips of the root network it is possible to form new agents within the root network which happens in the stage parenting coded in light blue. Additionally, the agent right before a branch is in the stage “branch” illustrated with yellow. Finally the grey frame at every agent represents the third growth process secondary thickening.

All properties of the agent forming the hairy root network are outlined in Table 1 and can be grouped into two clusters: physical parameters such as length, width, surface and volume but also concentrations and capacities for nutrients. Consequently, the stage every agent is currently in is also a member property.

#### Design concepts

Starting point for the modeling activities was images of hairy roots cultured on agar plates. The growth characteristics should be mathematically described. An agent-based description system was found to be suitable. Nevertheless, the correct implementation of an agent in the given hairy root network needed to be determined. Figure 2a shows as small hairy root network sample where in Fig. 2b a typical branching point is marked and enlarged in part c. To derive a suitable data structure this part of the network is cut into

**Table 1** List of used state variables as properties of each agent with unit and short description

Member property/state variable	Unit	Description
dPhi	l	Local curvature of a rootElement
width	cm	Width of a rootElement
length	cm	length of a rootElement
surface	cm <sup>2</sup>	Surface of a rootElement derived from its length and width
volume	cm <sup>3</sup>	Volume of a rootElement derived from its length and width
conSecMetab	l/cm <sup>3</sup>	Concentration of secondary metabolite in a rootElement
nutrientCapacity	mg	Maximum capacity of (a) nutrient of a rootElement
nutrientAmount	mg	Amount of nutrient currently present in a rootElement
oxygenAmount	mg	Maximum capacity of oxygen of a rootElement
oxygenCapacity	mg	Amount of nutrient currently present in a rootElement
lifestage		Current stage of a rootElement in the stage machine

small pieces each representing a cluster of cells (see Fig. 2d). In the model this is the smallest individual part and therefore the agent in this agent-based model and is referenced as rootElement. When looking at the centerpiece in Fig. 2e this rootElement is linked to three other rootElements. Chains of rootElements from one branching point to another or to a root network tip are considered segments. For geometrical and transportation purposes information will be exchanged between linked agents. In Fig. 2f1, e.g., nutrient fluxes to and from a rootElement to another are represented by arrows while geometrical values such as length, width and concentration of a secondary metabolite are visualized in Fig. 2f2. Generally, the geometry of every rootElement

is represented as a frustum and properties like surface and volume are derived from that.

As outlined above, the core component of the simulator is the rootElements; these agents collectively comprise the simulated organism. Their instances are then arranged in the form of a sparse or incomplete binary tree to define the root organism. So at least a link to the parent agent exists. This structure makes it possible to refer each instance to its neighboring agent for the simulation of transport processes, and primarily affects the self-replicating behavior of the organism as a whole. To model the formation of branching points, two levels of agents of the rootElements were defined: the main strand of the hairy root culture (Fig. 1, dark green agent also called branch1) and the offshoot (Fig. 1, light green agent also called branch2). This approach is based on the idea of a parent strand that periodically produces a branching daughter strand that itself again represents a main strand for eventually generated branches. The term nutrient contains data referring to the abundance of the carbon source (in this case, glucose) that is turned into biomass. Furthermore, oxygen is needed for biomass production and growth. It is treated as a nutrient which has a high concentration above the agar and a very low concentration in the medium. Implemented transport processes include diffusion from air into the agar and from air and agar into the rootElements.

The instances of rootElement provide all of the relevant and available information on the hairy root culture. This information can be accessed using a large set of methods. In general, each instance of rootElement draws information governing its metabolism and determines threshold values for its development and behavior from static members (which are typically constants, such as the temperature) or by calling appropriate functions (e.g., the distance to the nearest branching point).

The most important method available to the rootElements is the time-step method. Calling this method on the original rootElement of the root organism, the

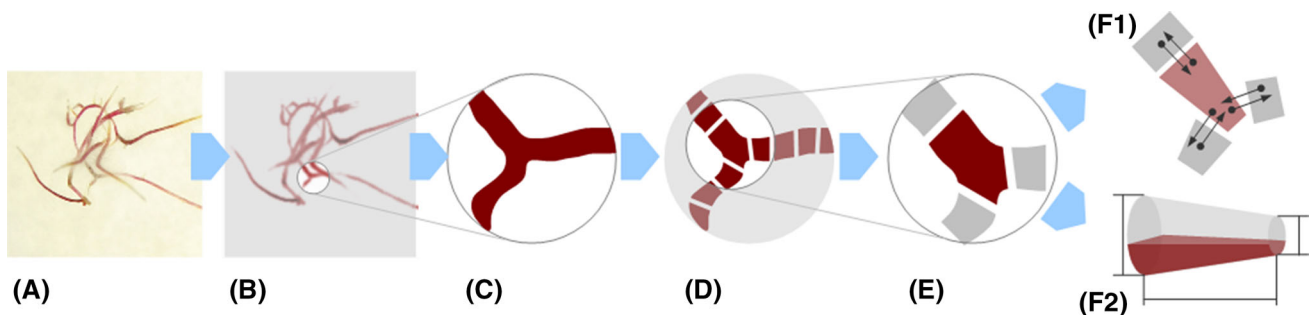


**Fig. 2** Derivation of the hairy root model architecture and data structure from the root network (a) to the single agent, its properties and interactions (f)



structural root of the binary tree with no parent, further referred to as “origin”, forces the simulation to advance by incrementing the time variable.

### Details

Due to the nature of the used recursive simulation approach it is necessary to start the simulation under defined conditions. The simulation needs to be initialized with a distinct original segment or a seed that has pre-defined, experimentally determined geometrical parameters and a direction of growth that follows a Gaussian distribution (see Table 2 for parameters `branchaxisPRandomAtStart`, `startLength`, `startWidth`). This original `rootElement` is placed on top of the medium at the time-step  $t_0$ .

Generally, there are three types of parameters available in terms of their origin. The term “measured” refers to that the value is directly derived from experimental data, while

the term “constructed” to a value that has been derived from a set of experiments. Finally, several parameters are needed to be fitted to match global experimental results. Once a simulation starts every change to a `rootElement` is based on a parameter from Table 2. Consequently, the stability in the curvature of adjoined `rootElement` is controlled by the parameter `inheritDPhi` and the balance between the nutrient concentration and an agent’s volume is defined by the rate of the `nutrientVolumeFactor`. To determine when a new branch has to be formed specific probabilities such as the `intercalaryLevel` have been implemented.

As explained in “Design concepts”, the root network containing the `rootElement`s supplied with nutrients (in this case glucose) and oxygen for growth. To reflect what happens in a real Petri dish several diffusion processes need to be considered. The nutrient reservoir is implemented as a 3D scalar field supported through a linear interpolated equidistant 3D-grid locally providing a limited

**Table 2** List of the numerical parameters used to simulate *Beta vulgaris* hairy root growth

Parameter	Value	Unit	Description	Source
<code>maxConcGrad</code>	100	1	Maximum concentration gradient	Fitted
<code>maxNutrFlow</code>	1.0	$\text{mg cm}^{-2} \text{h}^{-1}$	Maximum flow of nutrient into agents and between agents	Fitted
<code>builtSecMetab</code>	50.0, 5.0*	h	Production of secondary metabolites	Fitted
<code>minLength</code>	0.1	cm	Minimum length of an agent	Constructed
<code>maxLength</code>	0.5	cm	Maximum length of an agent	Constructed
<code>minWidth</code>	0.02	cm	Minimum width of an agent	Constructed
<code>startWidth</code>	0.06	cm	Initial width of the original agent	Measured
<code>startLength</code>	1.4	cm	Initial length of the original agent	Measured
<code>branchaxisPRandomAtStart</code>	0.0, 0.02*	°	Normal of agent growth direction	Fitted**
<code>inheritDPhi</code>	0.8, 0.2*	1	Angle alteration for branch1 curvature	Fitted
<code>newBranchWidthRandom</code>	2 <code>minWidth</code> , 0.05*	1	Sets width of a newly formed agent	Fitted
<code>inheritWidthRandom</code>	0.92, 0.05*	1	Alters width a joined agents	Fitted
<code>widthGrowthFactor</code>	0.001052, 0.0005	$\text{h}^{-1}$	Defines secondary thickening of agents	Measured
<code>nutrientVolumeFactor</code>	0.31151647	$\text{mg cm}^{-2} \text{h}^{-1}$	Conservative balance between nutrient concentration and agent volume	Measured
<code>specificLengthGrowthRate</code>	0.1122, 0.00163*	$\text{h}^{-1}$	Speed for tip growth	Measured
<code>growthCorrectionFactor</code>	3	1	Growth speed correction due to effects of higher order	Fitted
<code>intercalaryLevel</code>	0.2	1	Probability to create a branch2	Fitted, constructed
<code>intercalaryTransientlength</code>	0.05	1	Relative position in segment	Fitted, constructed
<code>addRandom</code>	0.0, 0.1*	1	Use as absolute factor for nutrient, oxygen and secondary metabolites	Fitted

\* Center and standard deviation of a frequency distribution

\*\* implementation detail (not measurable)

amount of carbon source to the `rootElements`. Diffusion processes are controlled by defined concentration gradients and a maximum flow of nutrients and oxygen between the environment and a `rootElement` (see Table 2 for parameters `maxConcGrad` and `maxNutr-Flow`). Oxygen is limited in the medium but unlimited on top of the agar.

While all necessary parameters are explained in Table 2 events are used to trigger a change of a `rootElement` or the creation of a new one. In this part the five sub-models used to simulate the evolution of a hairy root network are described in detail referring to the respective parts of Fig. 3.

The `branch1BuildEvent` is triggered if the `maxLength` is reached and sufficient nutrients and oxygen are available to the local `rootElement` which generates a new `branch1` (main strand). A `branch2` (offshoot) is created when the conditions of the `branch2Inter-calaryEvent` are met. This is controlled by the segment fragmentation expressed by a symmetric linear probability (see Fig. 3a), where  $i$  represents the inverse `Inter-calaryTransientLength` along the segment.

The `harvestAndSet` method, as the first of three steps in the time-step method, controls the nutrient and oxygen exchange between a `rootElement` and the environment, right after the external values have been applied and internal dependencies have been resolved as follows: an increasing capacity by age is determined using a linear expression (see Fig. 3b). Secondly, the transfer

process of nutrient and oxygen from the environment into the `rootElement` is triggered. This function calculates the optimum amount of nutrient available from the environment which also depends on the size of the surface of the `rootElement` and on the global temperature (see Fig. 3c). The `harvestAndSet` method is called recursively throughout the tree, what is causing a privileged bias to agents which can gain nutrients and oxygen first. This bias depends linear on the time-step size and therefore can be reduced to a minimum.

Once nutrients have been absorbed by the `rootElement`s concentration gradients need to be equalized between the agents. The function `nutrientBalancer` consists of a biased low pass filter that shares and mixes a fixed part of the local nutrient in neighboring `rootElement`s depending on the size of the time-step. Figure 3d illustrates this process by pooling the light blue share of nutrient from the two `rootElement`s and equally distributing them afterwards. The dark blue share remains in the `rootElement`. This function has to be called again on all branches until that the tree is traversed once.

Finally, the equalized resources in the `rootElement`s need to be turned into biomass. These processes are controlled by the last and third step, the `investResources` method and their application depends on the life stage the actual agent is currently in. In case the current stage is “extending” the possible addition in length is calculated based on the available amount of nutrient and oxygen and on the implemented growth speed (see Fig. 3e 1 → 2). If

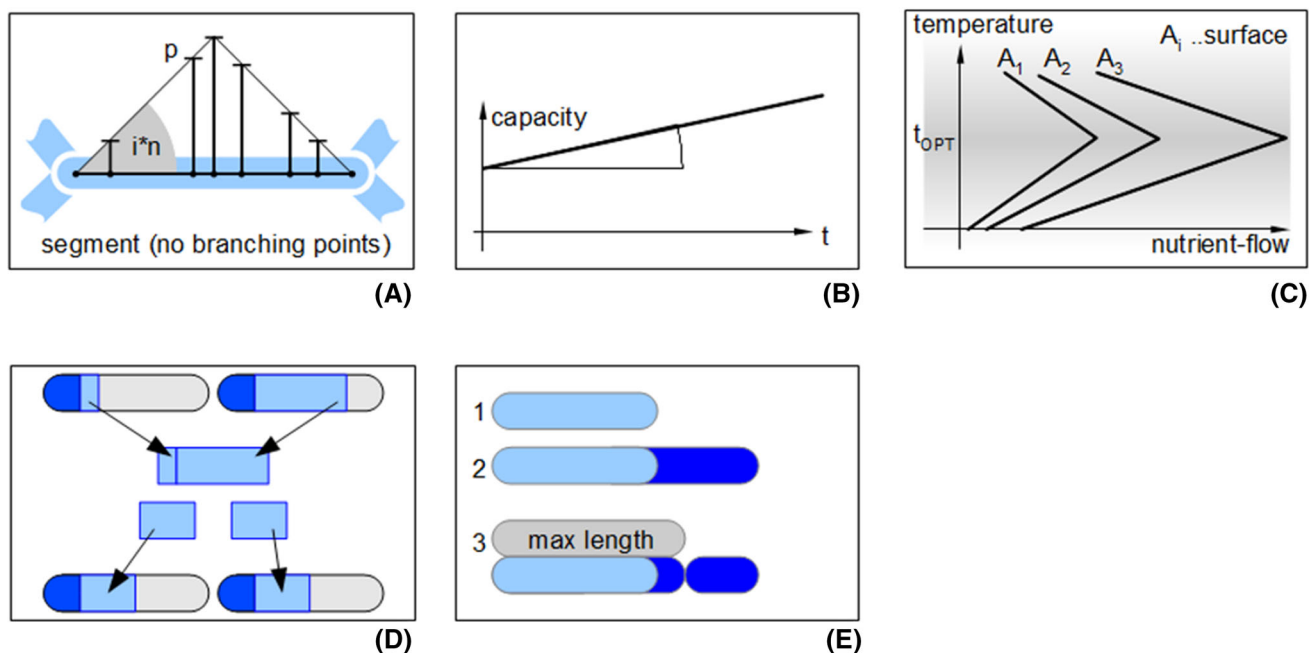


**Fig. 3** Composition of functional diagrams illustrating the used sub-models: **a** offshoot formation probability **b** agent’s nutrient and oxygen capacity increase dependent on age **c** calculation of amount of

nutrients to absorb from environment **d** low pass filtering to equalize nutrient and oxygen concentrations between agents **e** growth in length and formation of new branches

the maximum length as the structural maximum step width of this agent is reached a new `branch1` (main strand) is generated and this one will step its life stage forward to “parent”. After that the next agent will be handled (see Fig. 3e3).

If the current agent is in the stage “parent” no further growth in length will occur. Instead the available amount of nutrient and oxygen will be used for secondary thickening. Meanwhile `rootElements` in this life stage wait for the randomly triggered `branch2Intercalary-Event` that results in a new offshoot of the current agent.

The final life stage available to the agent is “branch”. During the `investResources` function in this life stage only secondary thickening and the age-dependent production of secondary metabolites (in this case the red pigments Betalains) occur. For an agent in this final life stage it is not possible to form new branches as they are already there.

At each time-step of the simulation, the above-mentioned single-way state machine is used to determine what actions should be taken for each `rootElement`. Therefore, it was necessary to implement several methods for measuring variables such as the total length or the volume of the root organism as a whole to determine when state transitions should occur. However, it was important to ensure that the tree as a whole was traversed only once when making decisions. In most cases, information on the properties of the root organism as a whole (e.g., the total root length, TRL) is required to make these decisions. To minimize computing time, care was taken to ensure that each manipulation step is performed exactly once per time-step for each `rootElement`.

It is important to understand that there is no such thing as a “central-control-instance” in this model because no such system exists in real root organism. Instead, each `rootElement` acts independently based on the data available from its properties and through its linked agents. In that manner the model is clearly agent-based and produces higher complexity through interacting simple lower units. Finally, the higher complexity is converging to the properties that can be seen in the real organism.

#### A 3D-visualization solution for displaying simulation results

After the first runs of the simulation it became apparent that the agent-based modeling approach as implemented in Java 1.7 was able to produce millions of elements in a matter of seconds on a typical personal computer. A powerful visualization strategy was, therefore, required to display the simulated results. It was decided that this would be best achieved using a real-time 3D-rendering engine, which was created using the backend of the OpenGL programming

language. Unfortunately, this means that the visualization system is hardly portable. The modeling structure that was used to describe the hairy root network and the clear structure of elements meant that there were several possible ways of optimizing the on-screen drawing process. In the system that was adopted, every element is drawn as a ruled surface that links the normal circles of each element to their child agents and the tip elements using a frustum. The lighting system is connected directly via the circle parameter and the color calculations. Because most of the trigonometric calculations are hard coded, the visualization solution is very fast and can draw around  $10^5$  elements with more than  $6 \times 10^6$  surfaces at more than 30 frames per second on a current high-end graphic adapter. The visualization system makes it possible to zoom in on specific regions of the root network in the Petri dish and to rotate the entire network to facilitate visual inspection (see Fig. 4).

In addition to displaying the simulated root network, the 3D engine makes it possible to visualize the nutrient matrix



**Fig. 4** Zoomable and rotatable 3D visualization of a hairy root network in a Petri dish. The colors of the network indicate the distribution and concentration of the secondary metabolite (*red* stands for high concentration, *grey* for low or no pigments present in the agent)

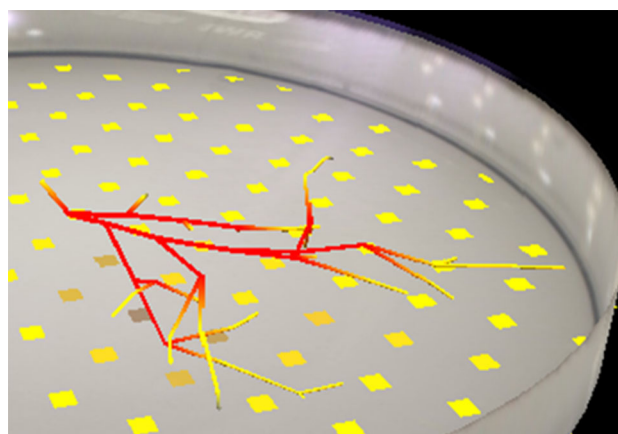


**Fig. 5** Zoomable and rotatable 3D visualization of a hairy root network showing the underlying nutrient matrix, in which the carbon source (*yellow*) is partially depleted (*grey*)



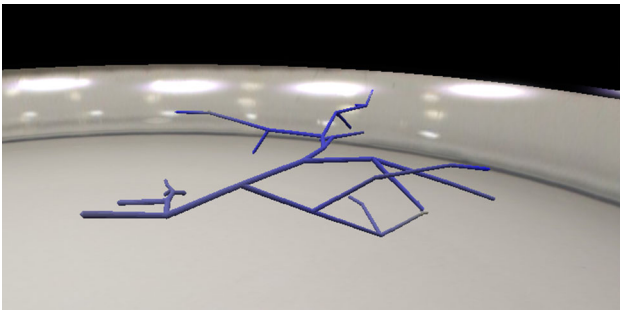


**Fig. 6** Zoomable and rotatable 3D visualization showing the distribution of oxygen within the hairy root network; *blue* indicates a high oxygen saturation while *grey* indicate low or no present oxygen in the agent

(see Fig. 5) and oxygen concentration (see Fig. 6) within the Petri dish at any given time-step. The distribution of nutrients (e.g., the carbon source) within the nutrient matrix is shown using a system of colored tiles: a deep yellow tile over a given location indicates no depletion of the carbon source, while a grey tile denotes an empty reservoir. The distribution of oxygen across the root network is shown by the color of the network itself; blue indicates an oxygen-saturated element, while grey indicates one that is low on oxygen.

Time-step specific and overall output of simulation results for further computation

The three-dimensional display of the simulated results facilitates their visual analysis. However, to enable quantitative comparisons between the simulated root networks, all of the characteristics of the growing process are recorded in several CSV documents. While the real experiments were only monitored twice per day, the simulation saves the characteristics of the root network after every time step (once every 4.8 h).

The output data from an individual simulation are stored in a folder that is named according to the date and time the simulation was run, and are subdivided into three kinds of data sheets. In keeping with the way experimental results are recorded, single segment data (e.g., SSL) are saved in one sheet per time-step. The time-step documents contain all of the individual segment metrics (i.e., segment length, width, volume, and pigment concentration) for each segment, and the mean values for each of these variables across the network as a whole are summarized in the file headers, together with the global data for the network—the total number of segments (TNS), total root length (TRL), total number of branching points (TBP), and mean distance between adjacent branching points.

In addition to the time-step documents, all of the mean segment data and global data are summarized in a special

sheet to facilitate investigations into the development of the network's average characteristics over time.

Finally, a special sheet is used to record the values of all the parameters used in the simulation, including the composition of the medium, the growth conditions, the randomization parameters, and details of vessel's geometry. These data are preserved to ensure that the simulation can be reproduced at a later date if required.

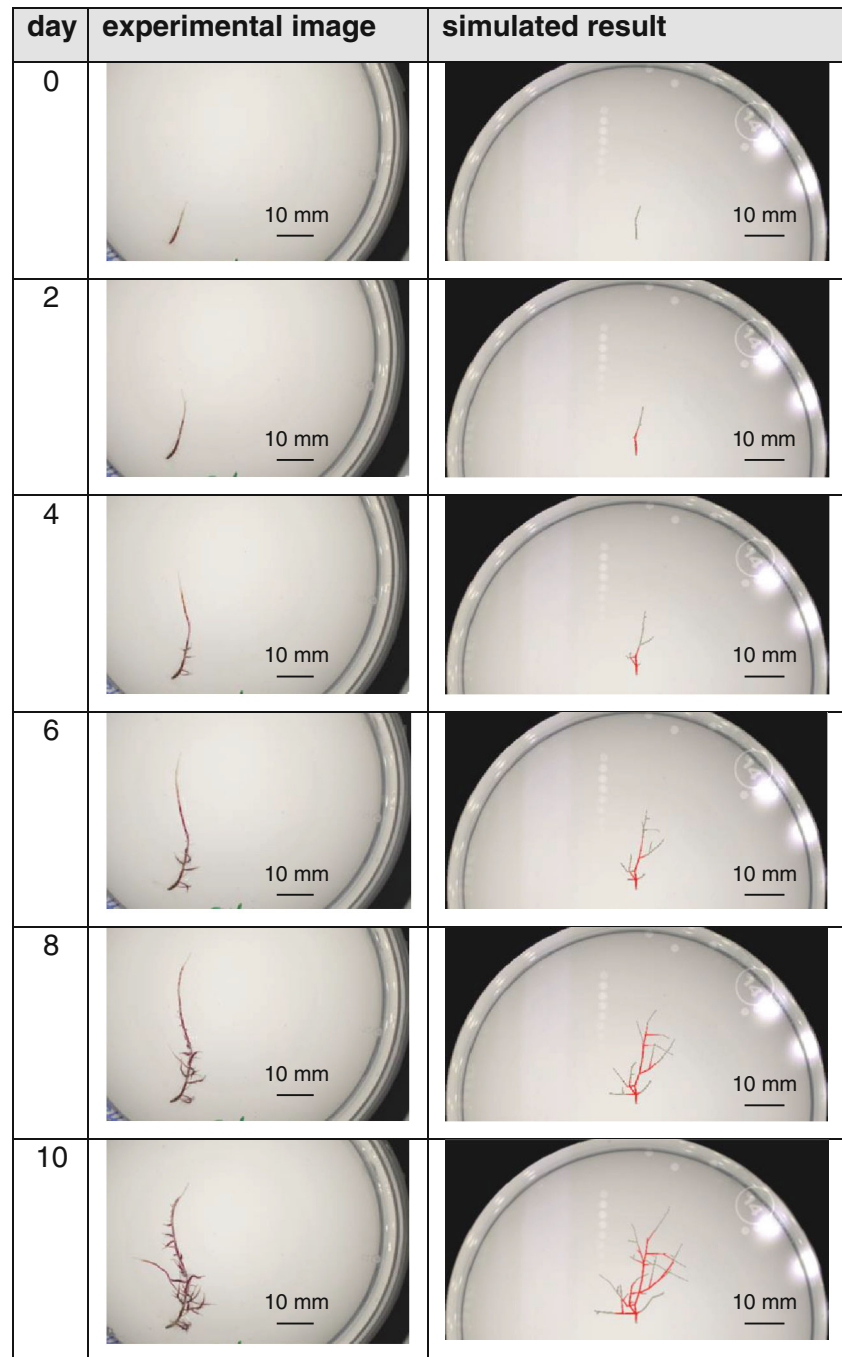
## Results and discussion

The implementation of the algorithms discussed in the preceding sections made it possible to simulate the growth of a *Beta vulgaris* hairy root networks and to compare the simulated results to experimental data. During the course of the computational work, experiments were conducted in which *Beta vulgaris* hairy root cultures were grown under conditions corresponding to those used in the simulations (see the “[Cultivation conditions](#)”). The structural parameters of the root organisms produced in these experiments were measured on six occasions and the resulting parameters (which are listed in Table 2) were used as inputs when setting up the simulations.

To facilitate comparisons between the experimental and simulated results, images of the experimental cultures taken at different time points are shown alongside 3D visualizations of the simulated results at equivalent points in their simulated timelines (see Fig. 7). In addition, the experimental and simulated results concerning the total number of segments (TNS) and total root length (TRL, see Fig. 8) were plotted together to illustrate the agreement between the two datasets. In general, the simulated results closely matched those observed experimentally, especially with respect to the total number of segments (TNS) and total root length (TRL). For all of these variables, the simulated values deviated from the mean experimental results by only 4–6 %. This suggests that the model accurately reproduces the structure of the growing hairy root cultures. It should be noted that one simulated time-step corresponds to a period of 4.8 h in the experiments.

Especially, the nutrient uptake of hairy root plant tissue systems has been investigated and modeled so far. While Ptashnyk et al. [9] derived a very complex macroscopic model description for the absorption of nutrients through a single hairy root branch without experimental proof, the presented simulation results (see Fig. 7) together with the experimental data show that a more simple, capacity-controlled absorption followed a discrete equalization is also an effective approach. Leitner et al. [23] in their model link the nutrient uptake to morphological and physiological properties of the hairy roots. The model presented herein follows this approach as it incorporates ages, several

**Fig. 7** Root network structures observed in experiments (*left-hand images*) and simulations (*right-hand images*); *red* colored segments indicate *red* pigment accumulation, *grey* segments correspond to low or no pigment accumulation



capacities and the life stage of a `rootElement` to determine its nutrient uptake rates which proved to recreate the natural behavior.

A continuous model for the global growth of hairy root biomass under varied feeding conditions presented by Bastian et al. [24] produces qualitatively comparable data to the simulator presented herein. However, their experiments were conducted in shaking flasks using *Ophiorrhiza mungos* Linn. Hairy roots thus make a direct comparison impossible.

The simulated results for the total root volume (TRV, see Fig. 9) were somewhat lower than those determined in the experiments. Unfortunately, the simulations cannot be modified to more closely reproduce the experimental results simply by manipulating the `growthCorrectionFactor` which is used to model the secondary thickening of older segments. There are several potential reasons for the discrepancy in this case. First, while the image recognition process delivers excellent results with respect to metrics such as branching point distribution and

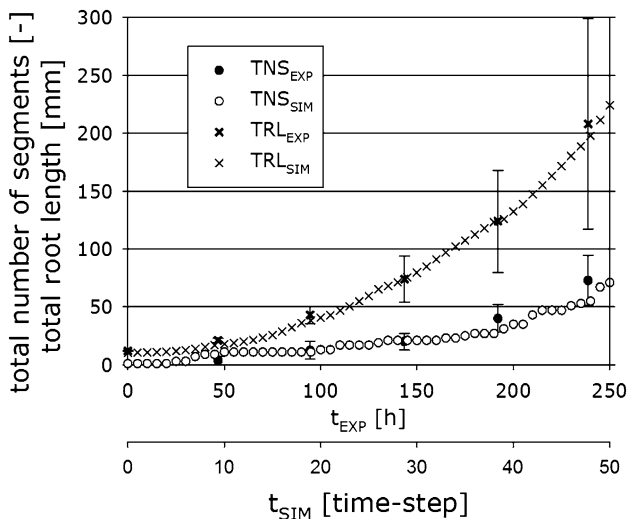


**Fig. 8** Comparison of experimental data (including standard deviations) and simulated results for the total root length (TRL) and total number of segments (TNS) of *Beta vulgaris* hairy roots on agar plates as a function of time

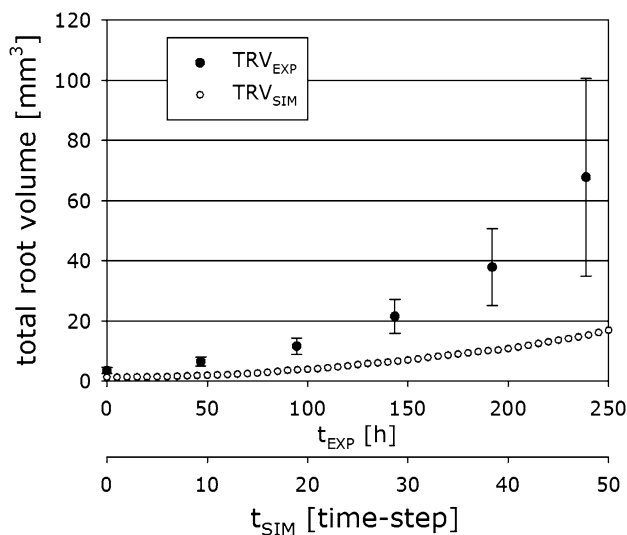


**Fig. 9** Comparison of experimental data (including standard deviations) and simulated results for the total root volume (TRV) of *Beta vulgaris* hairy roots on agar plates as a function of time

single segment length, the measured segment widths may be somewhat inaccurate. As discussed previously [21], the volume of the experimental segments is calculated by measuring their width and then treating the segment as a circular bistrum whose diameter at the thickest point is equal to the measured width. The volumes of the frusta are then integrated to estimate the volume of the segment. An unavoidable consequence of this approach is that even small errors in the measured segment width can generate large errors in the calculated segment volume. In addition, the volume of the segments may increase unusually rapidly when tip formation and elongation are down-regulated.

This would generate discrepancies between the TRV and the TRL, TNS and TBP values, which are consistent with the results obtained in this work.

**Conclusion and outlook**

For the first time, the agent-based model presented in this work makes it possible to comprehensively describe macroscopic growth processes in hairy root cultures and to give researchers an easily interpreted visual illustration of the simulated results. Currently, the described implementation of the model can be used to simulate the outcomes of experiments using standard cultivation conditions and medium compositions.

This version of the model and simulator can provide valuable information on the growth of hairy root tissue networks in Petri dishes, particularly with respect to their morphological development and the transport of nutrients and oxygen within the root organism. The simulated results make it possible to monitor nutrient depletion and oxygen uptake from the subordinated nutrition and oxygen matrices while also providing localized data on the oxygen and nutrient concentrations at a specific time-step during the culture’s morphological development. As such, the model and simulator can function as a virtual experimentator that can provide valuable predictions for use in the planning of practical experiments. Furthermore, the model can also be used for in silico testing of new medium compositions, since it is possible to vary the composition of the nutrient matrix and the consumption factors.

Finally, it should be noted that the current iteration of the model can be used to simulate a wide range of cultivation vessels, from Petri dishes (as used in this work) to bioreactors. In future, it would be desirable to determine the extent to which inheritance errors affect the tree structure. Overall, however, the results presented herein indicate that the new model is a powerful tool for studying non-regular biological structures such as hairy root networks, and offers considerable scope for further development.

**Acknowledgments** The authors gratefully acknowledge financial support from the European Social Fund (ESF) and the Free State of Saxony (project number 080938406).

**Conflict of interest** The authors have declared no commercial or financial conflict of interest.

**References**

1. Steingroewer J, Bley T, Georgiev V et al (2013) Bioprocessing of differentiated plant in vitro systems. Eng Life Sci 13:26–38. doi:10.1002/elsc.201100226

2. Weathers PJ, Towler MJ, Xu J (2009) Bench to batch: advances in plant cell culture for producing useful products. *Appl Microbiol Biotechnol* 85:1339–1351. doi:[10.1007/s00253-009-2354-4](https://doi.org/10.1007/s00253-009-2354-4)
3. Georgiev V, Ilieva M, Bley T, Pavlov A (2008) Betalain production in plant in vitro systems. *Acta Physiol Plant* 30:581–593. doi:[10.1007/s11738-008-0170-6](https://doi.org/10.1007/s11738-008-0170-6)
4. Mukundan U, Bhagwat V, Singh G, Curtis W (2012) Integrated recovery of pigments released from Red Beet hairy roots exposed to acidic medium. *J Plant Biochem Biotechnol* 10:67–69. doi:[10.1007/BF03263111](https://doi.org/10.1007/BF03263111)
5. Nussbaumer P, Kapetanidis I, Christen P (1998) Hairy roots of *Datura candida* D. aurea: effect of culture medium composition on growth and alkaloid biosynthesis. *Plant Cell Rep* 17:405–409. doi:[10.1007/s002990050415](https://doi.org/10.1007/s002990050415)
6. Boschke E, Bley T (1998) Growth patterns of yeast colonies depending on nutrient supply. *Acta Biotechnol* 18:17–27. doi:[10.1002/abio.370180103](https://doi.org/10.1002/abio.370180103)
7. Leduc M, Tikhomiroff C, Cloutier M et al (2006) Development of a kinetic metabolic model: application to *Catharanthus roseus* hairy root. *Bioprocess Biosyst Eng* 28:295–313. doi:[10.1007/s00449-005-0034-z](https://doi.org/10.1007/s00449-005-0034-z)
8. Morgan J (2002) Quantification of metabolic flux in plant secondary metabolism by a biogenetic organizational approach. *Metab Eng* 4:257–262. doi:[10.1006/mben.2002.0224](https://doi.org/10.1006/mben.2002.0224)
9. Ptashnyk M (2010) Derivation of a macroscopic model for nutrient uptake by hairy-roots. *Nonlinear Anal Real World Appl* 11:4586–4596. doi:[10.1016/j.nonrwa.2008.10.063](https://doi.org/10.1016/j.nonrwa.2008.10.063)
10. Cloutier M, Bouchard-Marchand É, Perrier M, Jolicoeur M (2008) A predictive nutritional model for plant cells and hairy roots. *Biotechnol Bioeng* 99:189–200. doi:[10.1002/bit.21543](https://doi.org/10.1002/bit.21543)
11. Han B, Linden JC, Gujarathi NP, Wickramasinghe SR (2004) Population balance approach to modeling hairy root growth. *Biotechnol Prog* 20:872–879. doi:[10.1021/bp0342304](https://doi.org/10.1021/bp0342304)
12. Dupuy L, Gregory PJ, Bengough AG (2010) Root growth models: towards a new generation of continuous approaches. *J Exp Bot* 61:2131–2143. doi:[10.1093/jxb/erp389](https://doi.org/10.1093/jxb/erp389)
13. Walther T, Reinsch H, Weber P et al (2011) Applying dimorphic yeasts as model organisms to study mycelial growth: part 1. Experimental investigation of the spatio-temporal development of filamentous yeast colonies. *Bioprocess Biosyst Eng* 34:13–20. doi:[10.1007/s00449-010-0442-6](https://doi.org/10.1007/s00449-010-0442-6)
14. Walther T, Reinsch H, Ostermann K et al (2011) Applying dimorphic yeasts as model organisms to study mycelial growth: part 2. Use of mathematical simulations to identify different construction principles in yeast colonies. *Bioprocess Biosyst Eng* 34:21–31. doi:[10.1007/s00449-010-0443-5](https://doi.org/10.1007/s00449-010-0443-5)
15. Walther T, Reinsch H, Grosse A et al (2004) Mathematical modeling of regulatory mechanisms in yeast colony development. *J Theor Biol* 229:327–338. doi:[10.1016/j.jtbi.2004.04.004](https://doi.org/10.1016/j.jtbi.2004.04.004)
16. Kreft J-U, Picioreanu C, Wimpenny JWT, van Loosdrecht MCM (2001) Individual-based modelling of biofilms. *Microbiology* 147:2897–2912
17. Lardon LA, Merkey BV, Martins S et al (2011) iDynoMiCS: next-generation individual-based modelling of biofilms. *Environ Microbiol* 13:2416–2434. doi:[10.1111/j.1462-2920.2011.02414.x](https://doi.org/10.1111/j.1462-2920.2011.02414.x)
18. Lindenmayer A (1968) Mathematical models for cellular interactions in development I. Filaments with one-sided inputs. *J Theor Biol* 18:280–299. doi:[10.1016/0022-5193\(68\)90079-9](https://doi.org/10.1016/0022-5193(68)90079-9)
19. Lindenmayer A (1968) Mathematical models for cellular interactions in development II. Simple and branching filaments with two-sided inputs. *J Theor Biol* 18:300–315. doi:[10.1016/0022-5193\(68\)90080-5](https://doi.org/10.1016/0022-5193(68)90080-5)
20. Murashige T, Skoog F (1962) A revised medium for rapid growth and bio assays with tobacco tissue cultures. *Physiol Plant* 15:473–497. doi:[10.1111/j.1399-3054.1962.tb08052.x](https://doi.org/10.1111/j.1399-3054.1962.tb08052.x)
21. Lenk F, Vogel M, Bley T, Steingroewer J (2012) Automatic image recognition to determine morphological development and secondary metabolite accumulation in hairy root networks. *Eng Life Sci* 12:588–594. doi:[10.1002/elsc.201200022](https://doi.org/10.1002/elsc.201200022)
22. Grimm V, Berger U, Bastiansen F et al (2006) A standard protocol for describing individual-based and agent-based models. *Ecol Model* 198:115–126. doi:[10.1016/j.ecolmodel.2006.04.023](https://doi.org/10.1016/j.ecolmodel.2006.04.023)
23. Leitner D, Klepsch S, Ptashnyk M et al (2010) A dynamic model of nutrient uptake by root hairs. *New Phytol* 185:792–802. doi:[10.1111/j.1469-8137.2009.03128.x](https://doi.org/10.1111/j.1469-8137.2009.03128.x)
24. Bastian P, Chavarría-Krauser A, Engwer C et al (2008) Modelling in vitro growth of dense root networks. *J Theor Biol* 254:99–109. doi:[10.1016/j.jtbi.2008.04.014](https://doi.org/10.1016/j.jtbi.2008.04.014)